Biophysical Journal
Article

Biophysical Society

DHHC5 Mediates β-Adrenergic Signaling in Cardiomyocytes by Targeting Gα Proteins

Jessica J. Chen,[1] Autumn N. Marsden,[1] C. Anthony Scott,[2] Askar M. Akimzhanov,[1] and Darren Boehning[3,*]
[1]Department of Biochemistry and Molecular Biology, McGovern Medical School at UTHealth, Houston, Texas; [2]Department of Pediatrics, Baylor College of Medicine, Houston, Texas; and [3]Department of Biomedical Sciences, Cooper Medical School of Rowan University, Camden, New Jersey

ABSTRACT S-palmitoylation is a reversible posttranslational modification that plays an important role in regulating protein localization, trafficking, and stability. Recent studies have shown that some proteins undergo extremely rapid palmitoylation/depalmitoylation cycles after cellular stimulation supporting a direct signaling role for this posttranslational modification. Here, we investigated whether β-adrenergic stimulation of cardiomyocytes led to stimulus-dependent palmitoylation of downstream signaling proteins. We found that β-adrenergic stimulation led to rapidly increased Gαs and Gαi palmitoylation. The kinetics of palmitoylation was temporally consistent with the downstream production of cAMP and contractile responses. We identified the plasma membrane-localized palmitoyl acyltransferase DHHC5 as an important mediator of the stimulus-dependent palmitoylation in cardiomyocytes. Knockdown of DHHC5 showed that this enzyme is necessary for palmitoylation of Gαs, Gαi, and functional responses downstream of β-adrenergic stimulation. A palmitoylation assay with purified components revealed that Gαs and Gαi are direct substrates of DHHC5. Finally, we provided evidence that the C-terminal tail of DHHC5 can be palmitoylated in response to stimulation and such modification is important for its dynamic localization and function in the plasma membrane. Our results reveal that DHHC5 is a central regulator of signaling downstream of β-adrenergic receptors in cardiomyocytes.

SIGNIFICANCE In the heart, β-adrenergic signaling plays an essential role in regulating contractile functions. Palmitoylation is a posttranslational modification that adds a 16-carbon palmitic acid to a cysteine residue. Multiple membrane-associated proteins in the β-adrenergic signaling pathway are palmitoylation targets. Here, we show that in response to agonist stimulation, Gα proteins can be palmitoylated. The kinetics of palmitoylation corresponds with cAMP production and positive inotropy. Mechanistically, we showed that the plasma membrane localized palmitoyl acyltransferase DHHC5 mediates agonist-induced palmitoylation and downstream functional changes. We adapted a novel, to our knowledge, in vitro assay to show that Gα proteins are direct substrates of DHHC5. We also showed that the C-terminal tail of DHHC5 is palmitoylated and it regulates the dynamic localization of DHHC5 in the plasma membrane.

INTRODUCTION

β-adrenergic receptor (β-AR) signaling is one of the central regulators of contractile function in the heart. Like other G-protein-coupled receptors, β-ARs associate with heterotrimeric G-proteins, composed of α, β, and γ subunits (1,2). Upon activation, β-ARs act as guanine nucleotide exchange factors and replace the GDP with GTP in G-protein α-subunits (3). Cardiac β-ARs associate with both Gαs and Gαi, which can stimulate or inhibit adenylyl cyclase, respectively (4,5). Adenylyl cyclase produces the secondary messenger cAMP, which activates multiple downstream effectors, including protein kinase A (PKA) (6,7). PKA phosphorylates many substrates that alter contractile functions, including ryanodine receptors, phospholamban, and cardiac troponin I (8–10). Given the crucial roles of β-AR signaling in regulating cardiac function, it is not surprising that this pathway is tightly controlled.

Multiple members of the β-AR signaling pathway undergo protein palmitoylation, a posttranslational modification that adds a 16-carbon palmitic acid to cysteine residues via a labile thioester bond. Protein palmitoylation is catalyzed by a class of enzymes termed palmitoyl acyltransferases (PATs). There are at least 23 mammalian PATs that share a conserved Asp-His-His-Cys (DHHC) domain that is

Submitted May 6, 2019, and accepted for publication August 19, 2019.

*Correspondence: boehning@rowan.edu

Jessica J. Chen and Autumn N. Marsden contributed equally to this work.

Editor: Joseph Falke.

https://doi.org/10.1016/j.bpj.2019.08.018

© 2019 Biophysical Society.

This is an open access article under the CC BY-NC-ND license (http://creativecommons.org/licenses/by-nc-nd/4.0/).

essential for PAT activity (11). Most of the DHHC PATs are localized to the Golgi apparatus and play crucial roles in the cycling of palmitoylated substrates between the Golgi apparatus and the plasma membrane. Recently, our lab showed that the plasma membrane-localized DHHC21 is responsible for rapid, agonist-induced palmitoylation of substrates downstream of the Fas death receptor in T-cells (12).

Small G-proteins such as Gα are classic palmitoylated proteins, and this modification is crucial for their plasma membrane targeting and subsequent functions (13,14). Studies in HeLa cells and primary hippocampal neurons suggested that Gα proteins can be palmitoylated by Golgi-localized DHHC3 and 7 (15). The enzymatic activity regulating Gα protein palmitoylation in cardiac tissue is incompletely understood. Recently, the β_2-AR was reported to be palmitoylated at two cysteine residues in cardiomyocytes in a PKA-dependent manner resulting in internalization after 20 min of isoproterenol (ISO) stimulation (16). In this study, it was found that the Golgi-associated DHHC9, 14, and 18 may mediate β_2-AR palmitoylation. For palmitoylation to regulate G-protein-coupled receptor signaling with kinetics consistent with a signaling role, presumably a plasma membrane localized DHHC enzyme should be activated. In cardiomyocytes, the plasma membrane localized DHHC5 enzyme has been shown to be concentrated in caveolae and regulate the dynamic palmitoylation of phospholemman, a regulatory subunit of the Na pump (17,18). Importantly, phospholemman palmitoylation is dependent upon PKA phosphorylation, indicating it is likely palmitoylated in a stimulus-dependent manner (17). Whether DHHC5 regulates the dynamic palmitoylation of other substrates after β-AR stimulation in cardiomyocytes is not known.

DHHC5 has a long C-terminal tail that is proposed to contain regulatory components that are crucial for substrate recognition, localization, activation, and other potential functions (18–20). Truncation mutants of DHHC5 showed that the region between amino acids 218 and 334 is necessary for recognizing substrates including phospholemman and flotillin 2 (18). In neurons, the tyrosine kinase Fyn phosphorylates DHHC5 at Y533 and stabilizes it at the synaptic site by forming a DHHC5/Fyn/PSD-95 protein complex (19). In adult mouse forebrain extracts, DHHC5 was found to be palmitoylated at three potential cysteines in the C-terminus tail, some of which are conserved in other DHHC enzymes (20). One recent study showed that DHHC6 is palmitoylated in the C-terminal tail by DHHC16, revealing a novel palmitoylation cascade to fine tune DHHC activities (21). However, the functional consequences of DHHC5 C-terminal tail palmitoylation remain largely unknown.

Here, we show that Gαs and Gαi are palmitoylated within minutes of β-AR activation in ventricular cardiomyocytes. The palmitoylation kinetics are temporally consistent with the downstream cAMP production and changes in contractility. Knockdown of DHHC5 significantly inhibits agonist-induced palmitoylation and downstream responses indicating that this enzyme is required for β-AR signaling in cardiomyocytes. Additionally, we show that DHHC5 is rapidly palmitoylated in the C-terminal tail in response to β-AR stimulation, and this modification regulates its retention within the plasma membrane. These results uncover a novel, to our knowledge, and essential palmitoylation-dependent signaling cascade downstream of β-ARs in cardiomyocytes.

MATERIALS AND METHODS

Antibodies, constructs, and reagents

Mouse monoclonal anti-Gαs was purchased from Millipore (MABN543; Burlington, MA). Rabbit monoclonal anti-Gαi/o and rabbit polyclonal anti-calnexin were purchased from Abcam (ab140125, ab22595; Cambridge, United Kingdom). Rabbit polyclonal anti-GRK2, anti-PKA C-α, anti-PKA RI-α/β were purchased from Cell Signaling (no. 3982, 4782, 3927; Danvers, MA). Rabbit polyclonal anti-AC5/6 was purchased from Millipore (ABS573). Rabbit polyclonal anti-DHHC5 was purchased from Proteintech (21324-1-AP; Rosemont, IL). Secondary antibodies conjugated to Alexa-488, Alexa-555 (Molecular Probes, Eugene, OR), peroxidase (Jackson ImmunoResearch, West Grove, PA), IRDye 680LT (LI-COR, Lincoln, NE), and 800CW (LI-COR) were used. The 3×FLAG-DHHC5 construct was a gift from Dr. Yusuke Ohno (Sapporo, Japan). DHHS5 mutant was built using q5 mutagenesis kit (New England BioLabs (NEB), Ipswich, MA) with primers 5′-TGATCATCACAGCCCCTGGGTG-3′ and 5′-AATTCCTCCA CACAGTTGTCAC-3′. DHHC5Δ236–245 deletion mutant was built using q5 mutagenesis kit (NEB) with primers 5′-AGTTCTCCAGCACCCAGG-3′ and 5′- GCCATTGGTGAAGGGATTC-3′. DHHC5 was cloned into the pmCherry-C1 vector from Clontech (now Takara Bio; 632524; Mountain View, CA) using the NEBuilder high-fidelity DNA assembly cloning (NEB; E5520) with primers 5′-CGACGGTACCGCGGGCCCGGGATC CATGCCCGCAGAGTCTGGAAAG-3′ and 5′-TCAGTTATCTAGATCCG GTGGATCCTCACACCGAAATCTCATAGGTGG-3′ following the manufacturer's protocol. Isoproterenol was purchased from Tocris (no. 1747; Bristol, United Kingdom) and was prepared fresh before use. Silencer Select DHHC5 small interfering RNAs (siRNAs; s168613, s168614), Gαs siRNAs (s128627-s128629), Gαi (s135492-s135494), calnexin siRNAs (s130760-s130762), and negative control medium GC duplex siRNA (12935112) were purchased from ThermoFisher Scientific (Waltham, MA). All other reagents were purchased at the highest possible purity from Sigma-Aldrich (St. Louis, MO).

Cell culture

The rat myoblast H9c2 and HEK293 cell lines were obtained from American Type Culture Collection and maintained according to American Type Culture Collection guidelines. Neonatal rat ventricular cardiomyocytes (NRVMs) were prepared from 1- to 2-day-old Sprague-Dawley rat pups, as previously described (22). Animals were purchased from Texas Animal Specialties (Humble, TX) and processed on the same day. Cardiomyocytes were plated on Primaria polystyrene plates (Corning, Corning, NY) or fibronectin-coated glass coverslips. Cells were initially maintained in a mixture of 40% Dulbecco's modified Eagle's medium, 40% Ham's F10 culture medium, and 20% fetal bovine serum. Forty-eight hours after plating, the media were replaced by a mixture of 50% Dulbecco's modified Eagle's medium and 50% Ham's F10 culture medium, supplied with human recombinant insulin (Gibco, Gaithersburg, MD), transferrin, and thyroxine (Sigma-Aldrich). Cytosine-B-D-arabino-furanoside hydrochloride (10 μM; Sigma-Aldrich) was present in all culture medium to prevent proliferation of fibroblasts or endothelial cells. Cardiomyocytes were transfected with Lipofectamine 3000 following the manufacturer's instruction. All siRNA knockdown experiments were carried out 48 h after transfection and within

1 week of initial plating. All overexpression experiments were carried out within 24 h after transfection. For DHHC5 knockdown and rescue experiments, only siRNA s168613 was used. All other experiments used both s168613 and s168614. The vertebrate animal procedures were approved by the Animal Welfare Committee at The University of Texas Health Science Center at Houston (UTHealth). For each assay, n represents the number of biological replicates from separate NRVM preps.

Verification of key antibodies

NRVMs were prepared and transfected with control and a mixture of three siRNAs targeting Gαs, Gαi, calnexin, and DHHC5 using Lipofectamine 3000 following the manufacturer's instructions. Cells were lysed 48 h after transfection. Western blotting confirmed that the commercial Gαs, Gαi, calnexin, and DHHC5 antibodies used in this study can detect the specific bands of the correct molecular weights, and these bands were reduced by siRNA-mediated knockdown of the respective transcripts (see Supporting Materials and Methods).

Preparation of adult left ventricular lysates

Frozen left ventricular tissue from adult rats was a gift of Dr. Karmouty-Quintana (UTHealth) and Drs. Youker and Amione-Guerra (Houston Methodist Hospital). Frozen tissue was homogenized and lysed in 1% β-D-maltoside in phosphate-buffered saline, supplemented with a protease inhibitor mixture (Roche 11873580001; Basel, Switzerland) and the acyl protein thioesterases inhibitor ML211 (10 μM; Cayman Chemicals, Ann Arbor, MI), followed by centrifugation (8000 × g, 5 min) to remove insoluble material. The cleared supernatant was stored at −80°C.

Acyl-biotin exchange

NRVMs were plated at a density of 1000 cells per mm^2 on 6-well plates. For control and DHHC5 knockdown experiments, the total amount of siRNA transfected was 30 pmol per 900,000 cells. NRVMs were stimulated with 10 μM ISO at room temperature for the indicated times, followed by scraping on ice in ice-cold lysis buffer. Cells were lysed in 1% β-D-maltoside or 0.5% sodium dodecyl sulfate (SDS) (for DHHC5 tail palmitoylation experiments) in phosphate-buffered saline, supplemented with a protease inhibitor mixture (Roche 11873580001) and acyl protein thioesterases inhibitor ML211 (10 μM; Cayman Chemicals). Acyl-biotin exchange (ABE) was performed as described previously with slight modifications (23). Briefly, proteins were precipitated by chloroform-methanol (CM) and incubated with 10 mM N-ethylmaleimide overnight at 4°C with gentle mixing. After three rounds of CM precipitation, samples were incubated with 400 mM hydroxylamine (HA (pH 7), freshly prepared) and 1 mM 1,6-hexane-bis-(3-[2-pyridyldithio]propionamide)-biotin for 50 min at 37°C with gentle mixing. When a minus-HA-treated sample was included, the sample was divided into two equal parts after the third precipitation, and NaCl was used instead of HA. After three rounds of CM precipitation, samples were incubated with streptavidin-agarose (Pierce Biotechnology, Waltham, MA) beads for at least 90 min up to 8 h at room temperature with gentle mixing. After four rounds of washes, bound proteins were eluted for 15 min at 80°C with shaking in 30 μL of elution buffer containing 1% β-mercaptoethanol and 2 mM dithiothreitol. The supernatants were transferred to new tubes and 20 μL of the samples were loaded onto a 4–20% gradient SDS polyacrylamide gel electrophoresis gel (BIO-RAD, Hercules, CA), followed by transfer to nitrocellulose membrane and immunoblotting. For quantification of palmitoylation levels, we utilized the endoplasmic-reticulum-resident protein calnexin as a control for protein palmitoylation. Calnexin palmitoylation levels were high in resting cells and marginally elevated after stimulation with ISO. Therefore, we used this protein to normalize and quantify the changes of palmitoylation levels in Gα proteins. Because of the very rapid kinetics of palmitoylation observed, we conclude that the changes in palmitoylation levels observed using ABE are consistent with regulated palmitoylation and depalmitoylation events rather than changes in total protein expression levels.

cAMP ELISA

For quantification of intracellular cAMP levels, NRVMs were plated at a density of 875 cells per mm^2 on 24-well plates. Forty-eight hours after transfection, cells were stimulated with 1 μM ISO and assayed using the direct cAMP enzyme-linked immunosorbent assay (ELISA) kit (Enzo, Farmingdale, NY) per the manufacturer's instructions. Each experiment was performed with at least three biological replicates.

Calcium imaging

NRVMs were plated at a density of 300 cells per mm^2 on fibronectin-coated glass coverslips. Cardiomyocytes were loaded with Fura-2 AM as described previously (22). Images were taken on a Nikon TiS inverted microscope (Tokyo, Japan) with a 40× oil immersion objective, and images were taken every second with a Photometrics Evolve electron-multiplying charged-coupled device camera (Tucson, AZ). ISO (10 μM) was added after 2 min of baseline recording. An oscillation was counted when the Fura-2 ratio rose 10% above the baseline ratio. Oscillation frequencies before and after ISO were calculated from five coverslips for each condition and mean ± standard error were plotted as described (22).

TIRF microscopy and analysis

NRVMs were plated at a density of 200–250 cells per mm^2 on fibronectin-coated glass coverslips and transfected with mCherry-DHHC5 or mCherry-DHHC5Δ236–245 for 24 h using Lipofectamine 3000. Images were taken on a Nikon Eclipse TiS TIRF microscope with a 60× apo TIRF oil immersion objective every 500 ms with an Andor Zyla scientific complementary metal oxide semiconductor camera (Belfast, Ireland). Beating cardiomyocytes were located and imaged for 3 min before treating with ISO (10 μM). Cells were continuously imaged for 10 min after stimulation. Images were analyzed using the TrackMate version 3.8.0 plugin for Fiji (24). We used the LoG detector for particles, and the thresholds were determined for each cell based on the fluorescence intensity. We used the linear assignment problem tracker (maximal distance 15 pixel; maximal frame gap 4) for particle tracking. All output files from TrackMate were used for data analysis. "Links in track statistics" data from each cell were exported from TrackMate as comma-separated value files and analyzed using custom Python scripts utilizing the pandas and NumPy packages for data analysis. Tracking files from individual cells were merged together into wild-type and mutant data frames. Time bins of 30 s were created for the 13-min experiment duration, and each row of the data frames, representing 0.5 s, were assigned to these time bins. Downstream analyses were carried out using these 30 s time bins. Particle lifetime analysis was performed by extracting all particles, which existed during a 30 s bin at the start of the experiment (time 0 min) and during one bin at the end of the experiment (time 10 min). The time that a particle existed (in frames) within this window was calculated for each particle and the normalized distribution was plotted along with the kernel density estimation (KDE) of the distribution (25). Plotting was performed in Python using the seaborn and matplotlib packages. The mean-square displacement (MSD) of every particle was calculated in Python using the following formula at each frame (n) (0.5 s) for a total of 60 frames (N) where x and y represent the coordinate position of the particle as determined by TrackMate:

$$MSD(n) = \frac{1}{N-n}\sum_{i=1}^{N-n}\left[(x_{n+i}-x_i)^2+(y_{n+i}-y_i)^2\right]$$

The MSD at each frame was plotted for a 30 s bin immediately before treatment (frames 300–360) and for a 30 s window 10-min posttreatment (frames 1560–1620). To analyze the number of particles for wild-type and Δ236–245 mutant proteins, "spots in track statistics" data for each cell were exported from TrackMate as comma-separated value files. For each cell, the number of particles that existed at each time point (0.5 s) were calculated and plotted. The line on the plot represents the mean between all cells at that point in time. The shaded area represents the 95% confidence interval.

Immunofluorescence staining

NRVMs were plated at a density of 250 cells per mm^2 on fibronectin-coated glass coverslips. Immunofluorescence staining was performed as described previously (22). Anti-DHHC5 was used at a concentration of 1:100. For the quantification of plasma membrane localization of DHHC5, the percentage of cells displaying clear plasma membrane localization from five separate fields were scored in a blinded manner.

In vitro DHHC5 activity assay

HEK293T cells were not transfected (control) or transfected with FLAG- or mCherry-tagged DHHS5 and DHHC5 using Lipofectamine 3000 for 18–24 h. Cells were lysed in lysis buffer containing 0.5% SDS, 150 mM NaCl, 50 mM Tris, 1% Triton, and 1 mM EDTA in the presence of protease inhibitor (Roche). Lysates are incubated at 4°C with rotation for 15 min, sonicated until no longer viscous, and diluted to a final concentration of 0.01% SDS. Rabbit monoclonal anti-FLAG (CST147935) or RFP-Trap (ChromoTek, Munich, Germany) were used to immunoprecipitate DHHS/C5. The reaction mix contains 500 nM recombinant human Gαs (Origene TP314318; Rockville, MD), nonmyristoylated rat Gαi proteins (gift of Dr. Carmen Dessauer and Dr. Tanya Baldwin) or recombinant human GAPDH (Abcam ab77109), 200 nM dithiothreitol, 300 μM n-dodecyl β-D-maltoside, and 5 μM palmitoyl CoA{N-[(7-nitro-2-1,3- benzoxadiazol-4-yl)-methyl]amino} (NBD; Avanti Polar Lipids, Alabaster, Alabama). For samples mixed with HA, a final concentration of 400 mM neutral HA is present in the reaction mix. Reactions were started by adding palm-CoA-NBD and kept shaking at 37°C. At the indicated time points, a portion of the reaction was taken out and stopped by adding 1% SDS and heating at 80°C for 15 min. Beads were boiled in the presence of 2% β-mercaptoethanol to check for DHHS/C5 proteins at the end of the reactions. All samples were run on 4–20% gradient gels, transferred, and imaged using a Chemi-Doc XRS+ system (BIO-RAD) with a blue epi-illumination and a 530/25 nm filter for the NBD signals. Standard Western blotting were used to check for the level of total substrate proteins.

RESULTS

ABE reveals known and novel, to our knowledge, palmitoylated proteins in the cardiac β-AR signaling pathway

Multiple methods have been developed to detect protein palmitoylation. The traditional method of metabolically labeling target proteins with [^{3}H]-palmitate is powerful, but not ideal for unbiased identification of multiple palmitoylation substrates. The efficiency of labeling is dependent on the ability of cells to incorporate labeled palmitate and the palmitate turnover rate of each individual protein (26). In addition, exogenous addition of palmitic acid to cells may drive nonphysiological processes including altering the acylation state of signaling proteins. More recently, ABE (Fig. S2) has been exploited as an efficient way of detecting the endogenous palmitoyl proteome in various tissues and organisms (23,27,28). The first step of ABE is blocking the free cysteine sites on proteins in cell lysates by using the thioreactive compound N-ethylmaleimide. Subsequently, the labile thioester bond at the palmitoylation site is cleaved using neutral HA exposing the free thiol group that can be subsequently biotinylated. After biotinylation, proteins are pulled down using streptavidin beads and eluted, followed by Western blotting to detect palmitoylated proteins. We used multiple rat cardiac cell types, including the myoblast cell line H9c2, neonatal rat ventricular myocytes (NRVMs), and adult murine left ventricular tissue for detection of palmitoylated proteins downstream of β-AR (Fig. 1, *A–C*). We used calnexin as a positive control for protein palmitoylation in all experiments (29,30). As expected, we found that Gαs and Gαi are palmitoylated in both cell types and in cardiac tissue. Additionally, we also identified G-protein-coupled receptor kinase 2 (GRK2), a negative regulator of β-AR signaling, as a novel, to our knowledge, palmitoylation target in H9c2 cells. Although GRK2 has never been shown as a palmitoylated protein, another member of the GRK family, GRK6, has been shown to be palmitoylated at the carboxyl-terminal domain in COS-7 cells (31). The PKA regulatory subunit showed low levels of palmitoylation in H9c2 cells, consistent with a previous proteomic study (32). However, given that there was little change in the palmitoylation levels of PKA compared to the control, we cannot conclusively state that the PKA regulatory subunit is palmitoylated. No palmitoylation was detected for other proteins downstream of β-ARs, including adenylyl cyclase 5/6 or PKA catalytic subunits (Fig. 1, *A–C*). Consistent with our ABE results in adult rat ventricular tissue (Fig. 1 *C*), a proteomic study in adult rat ventricular cardiomyocytes found that Gαs and Gαi are palmitoylated proteins (33). Interestingly, the study identified adenylyl cyclase 6, but not any other proteins listed in our study, as a potential palmitoylated protein. The purpose of these experiments using ABE in different rat cardiac cell types was to screen for potential palmitoylated proteins of interest in the β-AR signaling pathway. To more quantitatively study dynamic palmitoylation in cardiomyocytes, we focused on the NRVM model and assessed the palmitoylation levels of Gαs and Gαi proteins after agonist stimulation.

Activation of β-ARs induces rapid protein palmitoylation in cardiomyocytes

Previous studies indicate that stimulation of β-ARs increases the rate of turnover of palmitate groups on Gα (14,34,35). To examine whether Gαs and Gαi proteins are palmitoylated upon β-AR activation in cardiomyocytes, we stimulated primary NRVMs with the β-AR agonist

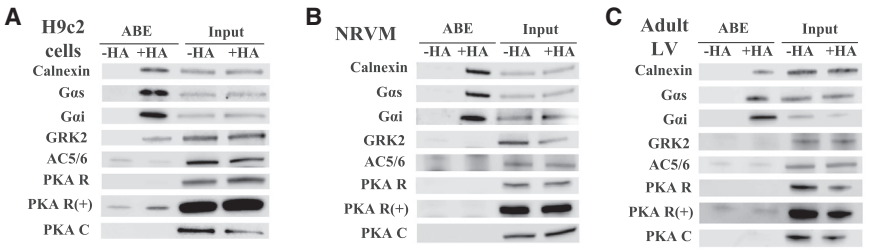

FIGURE 1 Palmitoylation of cardiac proteins as determined by acyl-biotin exchange (ABE). ABE was performed on H9c2 cells (*A*), neonatal rat ventricular myocytes (NRVMs) (*B*), and adult rat left ventricular tissue (*C*). Calnexin was used as a positive control. The absence of HA (−HA) was used as a negative control for nonspecific binding to streptavidin beads. Overexposure of the protein kinase A regulatory subunit (PKA R) blot is indicated with a (+). AC, adenylate cyclase; PKA C, PKA catalytic subunit.

ISO and collected lysates from 0 to 30 min. We then performed ABE to quantify palmitoylation levels of proteins of interest as in Fig. 1. We found that both Gαs and Gαi had significantly increased palmitoylation levels within a minute of ISO stimulation (Fig. 2, *A* and *B*). By 30 min, the palmitoylation levels of Gαs and Gαi were significantly reduced, suggesting a temporally distinct activation of acyl protein thioesterases. Interestingly, we also found that GRK2 can be palmitoylated after ISO stimulation (Fig. S3). The kinetics of GRK2 palmitoylation were characterized by increased levels at later time points compared to Gα proteins and were maintained throughout the 30 min time course (Fig. S3 *B*). These delayed kinetics may be functionally relevant to the negative regulatory role of GRK2 in the β-AR pathway. We next examined whether the agonist-induced palmitoylation is temporally consistent to downstream events mediating contractile functions. To test whether the kinetics of Gα palmitoylation correspond to downstream cAMP production, we measured intracellular cAMP levels in NRVMs after ISO stimulation. We found that cAMP levels increased within a minute of ISO stimulation and then decreased within 30 min (Fig. 2 *C*), which was temporally consistent with the kinetics of Gα palmitoylation (Fig. 2, *A* and *B*). ISO is known to induce positive inotropy in NRVMs (36). We used Fura-2 AM, a ratiometric calcium indicator, to monitor the intracellular calcium levels in spontaneously beating NRVMs. We observed an increase in calcium oscillation frequency (corresponding to beating frequency) within a minute of ISO stimulation, which, like cAMP production, was temporally consistent with the kinetics of Gα palmitoylation (Fig. 2 *D*). These correlative findings suggest that rapid palmitoylation of signaling proteins after β-AR stimulation may play a role in the assembly of the macromolecular β-AR signaling complex and efficient downstream modulation of cardiomyocyte contractility. To directly address this possibility, we targeted the enzymatic machinery potentially responsible for rapid palmitoylation of signaling proteins in cardiomyocytes.

The PAT DHHC5 mediates β-AR signaling in cardiomyocytes

We have previously shown that the plasma membrane localized DHHC enzyme DHHC21 is responsible for rapid agonist-induced palmitoylation of components of the Fas receptor pathway in T-cells (12). Therefore, we hypothesized that the DHHC enzyme that catalyzes the ISO-induced palmitoylation in cardiomyocytes must similarly be localized to the plasma membrane. In addition to DHHC21, DHHC5 is one of the few DHHC enzymes that has been shown to be at least partially plasma membrane localized (37). At the transcript level, DHHC5 is abundantly expressed in rat cardiomyocytes (18). We analyzed the localization of endogenous DHHC5 in NRVMs. Immunofluorescence staining showed that DHHC5 has Golgi/endoplasmic reticulum and plasma membrane localization (Fig. S4 *A*). To determine whether DHHC5 is responsible for ISO-induced palmitoylation in NRVMs, we used siRNA

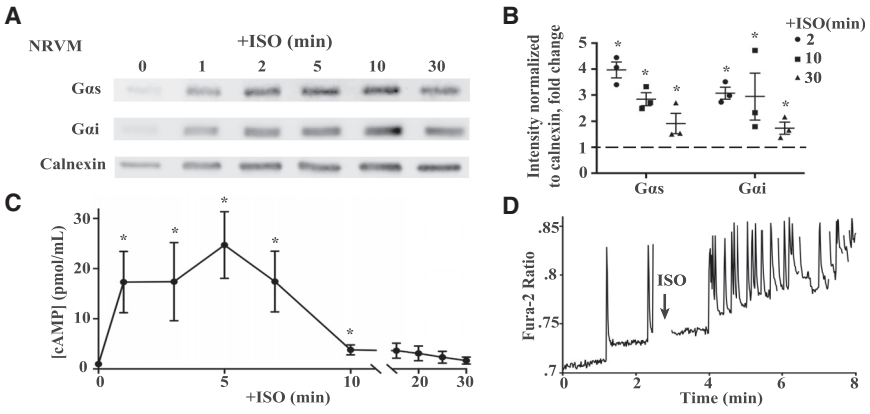

FIGURE 2 Isoproterenol (ISO) induces rapid and reversible palmitoylation of Gαs and Gαi in cardiomyocytes. (*A*) Neonatal rat ventricular myocytes (NRVMs) were treated with 10 μM ISO for the indicated times. ABE was used to detect palmitoylation levels. Calnexin, which has a relatively slow turnover of palmitoylation groups, was used to normalize turnover rates assessed by ABE. (*B*) Fold changes of palmitoylation levels of Gαs and Gαi normalized to calnexin at the indicated time points compared to 0 min ($n = 3$) are shown. (*C*) NRVMs were treated with 10 μM ISO for indicated time points, and intracellular cAMP concentration was measured using ELISA ($n = 5$). (*D*) A representative single-cell trace of the Fura-2 ratio in a NRVM cell treated with 10 μM ISO at the indicated time point is shown. *$p < 0.05$ (paired *t*-test).

to knock down DHHC5 in NRVMs (Fig. S4 *B*). We confirmed that total protein levels of GAPDH, Gαs, Gαi, and calnexin are not affected by DHHC5 knockdown (Fig. S4, *C–E*). We then performed ABE and found that agonist-induced palmitoylation of Gαs and Gαi is undetectable in DHHC5 knockdown cells (Fig. 3, *A* and *B*). Next, we determined whether DHHC5 activity is required for signaling downstream of ISO stimulation in NRVMs. We found that DHHC5 knockdown cells have diminished levels of cAMP production after ISO stimulation (Fig. 3 *C*). Additionally, we found that DHHC5 knockdown cells no longer have an increased calcium oscillation frequency in response to ISO stimulation (Fig. 3 *D*). These data indicate that DHHC5 is essential for signaling through the β-AR pathway in cardiomyocytes, and this is likely mediated at least in part by regulating the palmitoylation state of Gα proteins. To address whether our observation in cardiomyocytes are due to Gαs and Gαi being direct substrates of DHHC5, we utilized an in vitro assay to test DHHC5 enzymatic activity in the presence of recombinant protein substrates.

DHHC5 palmitoylates Gαs and Gαi in vitro

A previous study described an in vitro palmitoylation assay using a fluorescently labeled palmitoyl-CoA analog, palmitoyl CoA-NBD, to demonstrate that purified human DHHC20 and zebrafish DHHC15 can robustly palmitoylate *Legionella* ubiquitin ligase GobX and human SNAP25B, respectively (38). We overexpressed FLAG-tagged human DHHC5 or the catalytically inactive form of DHHS5 in HEK293 cells, immunoprecipitated DHHC/S5, and performed an on-bead enzymatic assay using palmitoyl CoA-NBD. To establish that the NBD fluorescent signal is attached to the substrates via thioester bonds, we added HA to the reaction mix as a negative control. For both no enzyme and catalytically inactive DHHS5 controls, we observed some level of autoacylation of Gα proteins, which has been reported in previous studies using [^{3}H]Palmitoyl-CoA in vitro (Fig. 4, *A* and *B*; (39)). In the presence of DHHC5, the rate of Gαs and Gαi palmitoylation was significantly accelerated (Fig. 4, *A* and *B*; quantification in

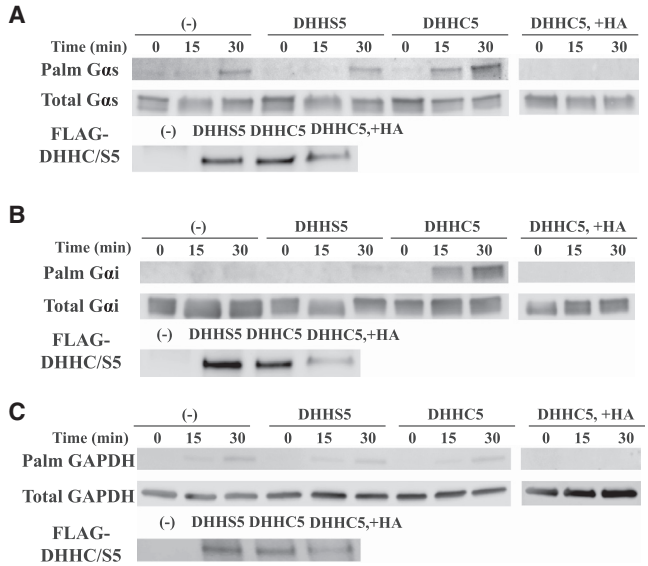

FIGURE 4 Gαs and Gαi are direct substrates of DHHC5. Palmitoylation of recombinant Gαs (*A*), Gαi (*B*), and GAPDH (*C*) in vitro with mock immunoprecipitation (−), catalytically inactive form of DHHC5 (DHHS5), and DHHC5 are shown. As a negative control, HA was added to cleave all thioester bonds. DHHC total input as determined by Western blotting is shown below the palmitoylation panels.

Fig. S5). In contrast, the known palmitoylated protein GAPDH (40) showed no increased palmitoylation in the presence of DHHC5, indicating substrate specificity (Figs. 4 *C* and S5 *D*). Additionally, an N-terminal mCherry-fused variant of DHHC5 performed similarly to the FLAG-tagged variant, validating that N-terminal tags do not appreciably impact enzymatic activity or substrate recognition of this enzyme (Fig. S5, *A–C*).

The C-terminal tail of DHHC5 is palmitoylated upon stimulation of β-ARs to modulate downstream signaling in cardiomyocytes

DHHC5 contains a very long C-terminal tail that can be a target for posttranslational modifications to modulate enzyme structure/function ((Fig. 5 *A*); (41)). Three potential

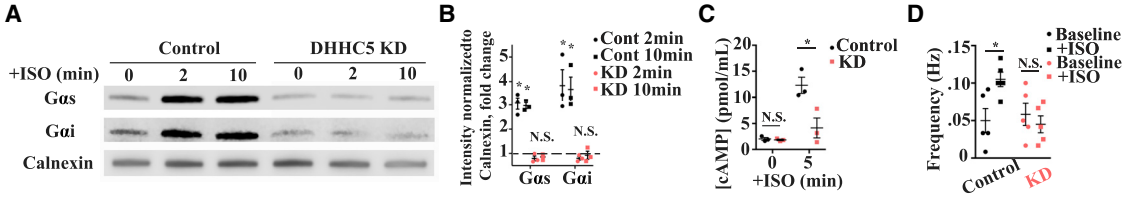

FIGURE 3 DHHC5 is required for signaling downstream of β-adrenergic receptor (β−AR) stimulation in cardiomyocytes. (*A*) Palmitoylation of Gαs, Gαi, and calnexin in control (Cont) and DHHC5 knockdown (KD) are shown. NRVMs treated with 10 μM ISO for the indicated time points are shown. (*B*) Fold changes of palmitoylation levels of Gαs and Gαi normalized to calnexin at the indicated time points compared to 0 min ($n = 3$) are shown. (*C*) Quantification of cellular cAMP levels before and after ISO (5 min) in Cont (*black*) and DHHC5 KD (*red*) NRVMs ($n = 3$) are shown. (*D*) Quantification of beating frequency monitored by Fura-2 before (baseline) and after ISO (+ISO) in Cont (*black*) and KD (*red*) cells ($n = 5$) is shown. *$p < 0.05$ (paired *t*-test). N.S. = not significant. To see this figure in color, go online.

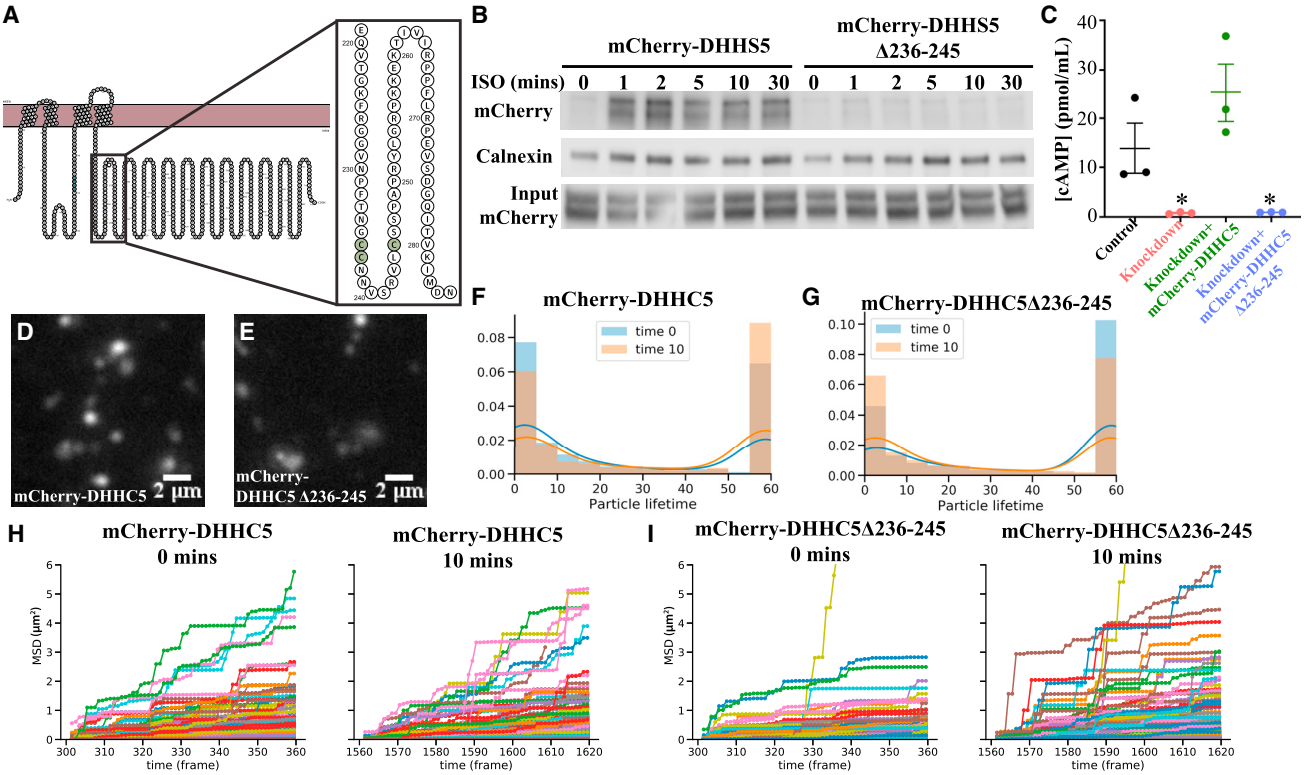

FIGURE 5 Palmitoylation of the C-terminal tail of DHHC5 regulates stimulation-dependent plasma membrane motility. (*A*) A schematic of DHHC5 created using Protter (41) is shown. Three potential palmitoylation sites within the tail are highlighted in green. (*B*) Palmitoylation of mCherry-DHHS5 and mCherry-DHHS5Δ236–245 in NRVMs treated with 10 μM ISO for the indicated time points is shown. Calnexin was used as positive control. (*C*) Quantification of cellular cAMP levels in control (*black*), knockdown (*red*), and knockdown and rescue with either mCherry-DHHC5 (*green*) or mCherry-DHHC5Δ236–245 (*blue*) in NRVMs are shown. TIRF images of live NRVM transfected with mCherry-DHHC5 (*D*) and mCherry-DHHC5Δ236–245 (*E*) are shown (also see Videos S1 and S2). (*F* and *G*) A histogram with KDE of the lifetime of particles at 0 (*blue*) and 10 min (*orange*) after ISO stimulation is shown. (*H–I*) Mean-square displacement (MSD) is shown in 30 s windows of particles that exist continuously from 0 to 10 min of ISO stimulation. Each line represents one particle. $n = 377$ for mCherry-DHHC5 (*F* and *H*) and $n = 221$ for mCherry-DHHC5Δ236–245 (*G* and *I*). *$p < 0.05$ (paired *t*-test, $n = 3$). To see this figure in color, go online.

palmitoylation sites in the C-terminal tail of DHHC5 have previously been identified in mouse forebrain extracts (Fig. 5 *A*, highlighted in *green*) (20). To determine if these sites are palmitoylated in NRVMs, we removed all three potential palmitoylation sites by deleting amino acids 236–245 (referred to as Δ236–245). DHHC enzymes are autocatalytically modified at the active site with palmitate (42); thus, we performed an ABE time course on the catalytically dead mCherry-DHHS5 and mCherry-DHHSΔ236–245 to only examine palmitoylation in the C-terminal tail. We found that DHHS5 is palmitoylated within 1 min upon ISO stimulation, whereas this is lost in the DHHSΔ236–245 mutant (Fig. 5 *B*; quantified in Fig. S6 *A*). This indicates that the C-terminal tail of DHHC5 is very rapidly palmitoylated in this region upon β-AR stimulation. To address the functional outcomes of DHHC5 tail palmitoylation upon stimulation, we knocked down DHHC5 in NRVM and attempted to rescue downstream cAMP production with both wild-type mCherry-DHHC5 and mCherry-DHHC5Δ236–245 (Figs. 5 *C* and S7). We found that wild-type mCherry-DHHC5 restored cAMP production after ISO stimulation, whereas mCherry-DHHC5Δ236–245 failed to rescue cAMP production (Fig. 5 *C*). Therefore, we conclude that palmitoylation of the DHHC5 C-terminal tail is required for cAMP production downstream of the β-AR. We next tested the hypothesis that DHHC5 palmitoylation in the C-terminal tail leads to sequestration in membrane microdomains where it can assemble with other components of the β-AR signaling pathway to facilitate downstream signaling (43–45).

Palmitoylation of the C-terminal tail of DHHC5 regulates stimulation-dependent plasma membrane motility

To determine the effect of palmitoylation on DHHC5 membrane motility, we utilized total internal reflection fluorescence (TIRF) microscopy (46). We imaged live, beating NRVMs transfected with mCherry-DHHC5 and mCherry-DHHC5Δ236–245. Both proteins were expressed in the TIRF plane as laterally mobile puncta of various fluorescent intensities presumably representing either single molecules

or oligomers (Fig. 5, *D* and *E*; Videos S1 and S2; (47,48)). These localization patterns are consistent with the immunofluorescence data showing that DHHC5 is localized partially to the plasma membrane in NRVMs (Fig. S4 *A*). First, we confirmed that mCherry-DHHC5Δ236–245 can localize to the plasma membrane appropriately like the wild-type proteins, with a similar number of observed particles in the TIRF plane (Figs. 5, *D* and *E* and S6 *B*). We next examined the lifetime of mCherry-DHHC5 particles in the TIRF plane to examine whether there is stimulus-dependent removal or insertion of DHHC5 into the plasma membrane. To accomplish this, we used KDE analysis (49,50) to calculate the lifetime of particles before and after 10 min of ISO stimulation (Fig. 5, *F* and *G*). When comparing the particle distributions before and after ISO stimulation, we observed a shift to longer lived particles after β-ARs were activated (Fig. 5 *F*). In contrast, the mCherry-DHHC5Δ236–245 showed the opposite result (Fig. 5 *G*). Thus, ISO stimulation led to the stabilization of DHHC5 particles at the plasma membrane, an effect that was lost in the palmitoylation-deficient DHHC5 mutant.

TIRF imaging has been widely used to examine lateral mobility in multiple systems before and after various stimulations (51–53). We next examined the lateral mobility of DHHC5 in the plasma membrane before and after ISO stimulation. To quantify this, we calculated the MSD of all particles present before and after 10 min of ISO stimulation. MSD calculates the summation of particle movement over time (54). Stalling particles will show a straight horizontal line as a function of time, whereas those moving quickly will show a steep slope. We found that the MSD of mCherry-DHHC5 particles remains essentially unchanged before and after ISO stimulation, indicating no change in lateral mobility (Fig. 5 *H*). In contrast, the mCherry-DHHC5Δ236–245 particles have an increase in the MSD after ISO stimulation, indicative of increased mobility (Fig. 5 *I*). In total, these data indicate that DHHC5 is palmitoylated in the C-terminal tail after ISO stimulation (Fig. 5 *B*), leading to stabilization in the plasma membrane (Fig. 5, *F* and *H*). The DHHC5Δ236–245 mutant cannot be palmitoylated (Fig. 5 *B*), leading to decreased lifetime at the membrane and increased motility (Fig. 5, *G* and *I*), presumably reflecting increased ISO-stimulated removal from the TIRF plane. Thus, palmitoylation of the DHHC5 C-terminal tail is critical for maintaining the enzyme at the membrane after β-AR stimulation with potentially significant consequences for palmitoylation-dependent signaling cascades.

DISCUSSION

Rapid, agonist-induced palmitoylation in signaling transduction

Palmitoylation is the only reversible lipid modification, and a growing list of signaling proteins are known to undergo cycles of palmitoylation and depalmitoylation (55,56). Recently, our group showed that the tyrosine kinase Lck can be palmitoylated within a minute of Fas ligand stimulation in T-cells, suggesting that palmitoylation plays a key role in rapid signal transduction analogous to other posttranslational modifications such as phosphorylation (12). Multiple members of the Gα protein family, including Gαs and Gαi, have been shown to be palmitoylated in the N-terminus (13,34). In cell lines, overexpression of Gαs and Gαi palmitoylation mutants showed defects in membrane association (14,57). Stimulation of β-ARs in kidney fibroblast-like COS cells and S49 lymphoma cells did not lead to detectable changes in Gα protein palmitoylation levels using high-performance liquid chromatography (58), although an earlier study found that [^{3}H]palmitate had increased turnover after ISO stimulation (35). One possible explanation is that [^{3}H]palmitate loading only labels a small fraction of the total Gα pool, which cannot be detected using high-performance liquid chromatography. Additionally, another recent study in HEK cells observed redistribution of Gα proteins to internal membranes after ISO stimulation, and the authors suggested that such events are independent of the acylation-deacylation cycles (59). Recent advances in palmitoylation detection methods allow us to better study dynamic palmitoylation of endogenous Gα proteins with endogenous lipids and their functional outcomes in specific cell types. Our data demonstrate extremely rapid palmitoylation kinetics of Gα proteins after activation of the β-ARs and its temporal correlation with downstream events in cardiomyocytes. The requirement of palmitoylation for β-AR signaling were functionally demonstrated by transient knockdown of DHHC5, which reduced or eliminated the majority of downstream effects of ISO stimulation in cardiomyocytes.

DHHC5 is a novel, to our knowledge, regulator of cardiac functions

Few studies have examined the cellular function of DHHC5 and its link to human diseases. One of the known substrates of DHHC5 is the neuronal scaffolding protein PSD-95, which is enriched at postsynaptic sites in neurons (60). Mice homozygous for a hypomorphic allele of *zdhhc5* gene showed defects in learning and memory (60). Curiously, PSD-95 palmitoylation levels are not decreased in the hypomorphic mice, likely because PSD-95 can also be palmitoylated by other DHHC enzymes in neurons (61). The homozygous DHHC5 hypomorphic mice show partial lethality, suggesting its role in early development (60). Cardiomyocytes isolated from these mice showed reduced massive endocytosis, a process that happens during reoxygenation of anoxic hearts (62). Phospholemman and the cardiac Na/Ca exchanger were identified as potential substrates of DHHC5 in regulating massive endocytosis (62). Several other studies on cardiac functions of DHHC5 also focus on its substrate phospholemman in regulating sodium

pumps in adult ventricular myocytes (17,18). Our data identify the β-AR signaling, a pathway that is closely associated with heart failure and is a major therapeutic target in cardiovascular diseases, as a key target for the enzymatic action of DHHC5.

Lipid subdomains and β-adrenergic signaling transduction in the heart

Lipid subdomains have been proposed to create signaling centers to facilitate both signal propagation and inhibition. One of the lipid subdomains present within many cell types is caveolae. Within cardiomyocytes, caveolae are composed of caveolin-3, cholesterol, and sphingolipids. Caveolin proteins have been proposed to create a scaffold, allowing signaling complexes to form at the membrane. Multiple components of β-AR signaling have been identified in caveolae, such as β2-AR, Gαs, AC5/6 and Gαi (43–45), indicating that caveolae are central organizers of this pathway. DHHC5 itself has been shown to be present in caveolae, allowing for direct palmitoylation of phospholemman (18). Proteomic studies identified that palmitoylated proteins are predominantly found in caveolae, suggesting that this is a better predictor of caveolae localization than caveolin-binding motifs (32). Our findings that DHHC5 is palmitoylated in the C-terminal tail upon stimulation in cardiomyocytes implies that DHHC5 as well as its targets are enriched in caveolae to allow efficient signaling transduction.

In cardiomyocytes, little is known about DHHC enzyme regulation. Our findings highlight the central role of the C-terminal tail in modulating DHHC5 function in cardiomyocytes. In particular, we found that palmitoylation of the tail had dramatic effects on plasma membrane retention after activation of the β-AR pathway. The tail region is highly variable in the DHHC family of enzymes, indicating this region may be a central mediator of isoform-specific function and substrate recognition. Future studies will need to address how other posttranslational modifications such as phosphorylation affect DHHC5 function and downstream signaling.

SUPPORTING MATERIAL

Supporting Material can be found online at https://doi.org/10.1016/j.bpj.2019.08.018.

AUTHOR CONTRIBUTIONS

J.J.C., A.N.M., A.M.A., and D.B. designed the experiments. J.J.C. and A.N.M. conducted the experiments. J.J.C., A.N.M., C.A.S., and D.B. analyzed the data. All authors wrote and edited the manuscript.

ACKNOWLEDGMENTS

We thank Dr. Karmouty-Quintana (UTHealth, Houston) and Drs. Youker and Amione-Guerra (Houston Methodist Hospital) for kindly providing us with adult rat ventricular tissue. We thank Drs. Dessauer and Baldwin (UTHealth, Houston) for kindly providing us with recombinant Gαi proteins. We thank Dr. Seung-Hee (Sally) Yoo (UTHealth, Houston) for kindly providing us with GAPDH antibody. Finally, we thank Dr. Shane Cunha (UTHealth, Houston) for technical assistance with NRVM preparations.

This work was supported by National Institutes of Health grants R01GM081685 (D.B.) and R01GM115446 (A.M.A.) and American Heart Association Predoctoral Fellowship 18PRE33960153 (J.J.C.).

REFERENCES

1. Gilman, A. G. 1987. G proteins: transducers of receptor-generated signals. *Annu. Rev. Biochem.* 56:615–649.
2. Simon, M. I., M. P. Strathmann, and N. Gautam. 1991. Diversity of G proteins in signal transduction. *Science.* 252:802–808.
3. Hendriks-Balk, M. C., S. L. Peters, …, A. E. Alewijnse. 2008. Regulation of G protein-coupled receptor signalling: focus on the cardiovascular system and regulator of G protein signalling proteins. *Eur. J. Pharmacol.* 585:278–291.
4. Xiao, R. P. 2001. Beta-adrenergic signaling in the heart: dual coupling of the beta2-adrenergic receptor to G(s) and G(i) proteins. *Sci. STKE.* 2001:re15.
5. Rockman, H. A., W. J. Koch, and R. J. Lefkowitz. 2002. Seven-transmembrane-spanning receptors and heart function. *Nature.* 415:206–212.
6. Ishikawa, Y., S. Katsushika, …, C. J. Homcy. 1992. Isolation and characterization of a novel cardiac adenylylcyclase cDNA. *J. Biol. Chem.* 267:13553–13557.
7. Göttle, M., J. Geduhn, …, R. Seifert. 2009. Characterization of mouse heart adenylyl cyclase. *J. Pharmacol. Exp. Ther.* 329:1156–1165.
8. Lindemann, J. P., L. R. Jones, …, A. M. Watanabe. 1983. beta-Adrenergic stimulation of phospholamban phosphorylation and Ca2+-ATPase activity in guinea pig ventricles. *J. Biol. Chem.* 258:464–471.
9. Takasago, T., T. Imagawa, and M. Shigekawa. 1989. Phosphorylation of the cardiac ryanodine receptor by cAMP-dependent protein kinase. *J. Biochem.* 106:872–877.
10. Valdivia, L. A., H. Sun, …, T. E. Starzl. 1997. Donor-specific transfusion in the nude rat prolongs survival of subsequently transplanted hamster cardiac xenografts. *Transplant. Proc.* 29:928–929.
11. Fukata, M., Y. Fukata, …, D. S. Bredt. 2004. Identification of PSD-95 palmitoylating enzymes. *Neuron.* 44:987–996.
12. Akimzhanov, A. M., and D. Boehning. 2015. Rapid and transient palmitoylation of the tyrosine kinase Lck mediates Fas signaling. *Proc. Natl. Acad. Sci. USA.* 112:11876–11880.
13. Linder, M. E., P. Middleton, …, S. M. Mumby. 1993. Lipid modifications of G proteins: alpha subunits are palmitoylated. *Proc. Natl. Acad. Sci. USA.* 90:3675–3679.
14. Wedegaertner, P. B., D. H. Chu, …, H. R. Bourne. 1993. Palmitoylation is required for signaling functions and membrane attachment of Gq alpha and Gs alpha. *J. Biol. Chem.* 268:25001–25008.
15. Tsutsumi, R., Y. Fukata, …, M. Fukata. 2009. Identification of G protein alpha subunit-palmitoylating enzyme. *Mol. Cell. Biol.* 29:435–447.
16. Adachi, N., D. T. Hess, …, J. S. Stamler. 2016. S-palmitoylation of a novel site in the β2-Adrenergic receptor associated with a novel intracellular itinerary. *J. Biol. Chem.* 291:20232–20246.
17. Tulloch, L. B., J. Howie, …, W. Fuller. 2011. The inhibitory effect of phospholemman on the sodium pump requires its palmitoylation. *J. Biol. Chem.* 286:36020–36031.
18. Howie, J., L. Reilly, …, W. Fuller. 2014. Substrate recognition by the cell surface palmitoyl transferase DHHC5. *Proc. Natl. Acad. Sci. USA.* 111:17534–17539.

19. Brigidi, G. S., B. Santyr, …, S. X. Bamji. 2015. Activity-regulated trafficking of the palmitoyl-acyl transferase DHHC5. *Nat. Commun.* 6:8200.

20. Collins, M. O., K. T. Woodley, and J. S. Choudhary. 2017. Global, site-specific analysis of neuronal protein S-acylation. *Sci. Rep.* 7:4683.

21. Abrami, L., T. Dallavilla, …, F. G. van der Goot. 2017. Identification and dynamics of the human ZDHHC16-ZDHHC6 palmitoylation cascade. *eLife.* 6:e27826.

22. Garcia, M. I., A. Karlstaedt, …, D. Boehning. 2017. Functionally redundant control of cardiac hypertrophic signaling by inositol 1,4,5-trisphosphate receptors. *J. Mol. Cell. Cardiol.* 112:95–103.

23. Roth, A. F., J. Wan, …, N. G. Davis. 2006. Global analysis of protein palmitoylation in yeast. *Cell.* 125:1003–1013.

24. Tinevez, J. Y., N. Perry, …, K. W. Eliceiri. 2017. TrackMate: an open and extensible platform for single-particle tracking. *Methods.* 115:80–90.

25. Jones, E., T. Oliphant, …, P. Peterson. 2001. SciPy: open source scientific tools for Python. http://www.scipy.org/.

26. Drisdel, R. C., and W. N. Green. 2004. Labeling and quantifying sites of protein palmitoylation. *Biotechniques.* 36:276–285.

27. Kang, R., J. Wan, …, A. El-Husseini. 2008. Neural palmitoyl-proteomics reveals dynamic synaptic palmitoylation. *Nature.* 456:904–909.

28. Dowal, L., W. Yang, …, R. Flaumenhaft. 2011. Proteomic analysis of palmitoylated platelet proteins. *Blood.* 118:e62–e73.

29. Dallavilla, T., L. Abrami, …, F. G. van der Goot. 2016. Model-driven understanding of palmitoylation dynamics: regulated acylation of the endoplasmic reticulum chaperone calnexin. *PLoS Comput. Biol.* 12:e1004774.

30. Lynes, E. M., M. Bui, …, T. Simmen. 2012. Palmitoylated TMX and calnexin target to the mitochondria-associated membrane. *EMBO J.* 31:457–470.

31. Stoffel, R. H., R. R. Randall, …, J. Inglese. 1994. Palmitoylation of G protein-coupled receptor kinase, GRK6. Lipid modification diversity in the GRK family. *J. Biol. Chem.* 269:27791–27794.

32. Gould, N. S., P. Evans, …, H. Ischiropoulos. 2015. Site-specific proteomic mapping identifies selectively modified regulatory cysteine residues in functionally distinct protein networks. *Chem. Biol.* 22:965–975.

33. Wypijewski, K. J., M. Tinti, …, W. Fuller. 2015. Identification of caveolar resident proteins in ventricular myocytes using a quantitative proteomic approach: dynamic changes in caveolar composition following adrenoceptor activation. *Mol. Cell. Proteomics.* 14:596–608.

34. Degtyarev, M. Y., A. M. Spiegel, and T. L. Jones. 1993. The G protein alpha s subunit incorporates [3H]palmitic acid and mutation of cysteine-3 prevents this modification. *Biochemistry.* 32:8057–8061.

35. Wedegaertner, P. B., and H. R. Bourne. 1994. Activation and depalmitoylation of Gs alpha. *Cell.* 77:1063–1070.

36. Proven, A., H. L. Roderick, …, M. D. Bootman. 2006. Inositol 1,4,5-trisphosphate supports the arrhythmogenic action of endothelin-1 on ventricular cardiac myocytes. *J. Cell Sci.* 119:3363–3375.

37. Ohno, Y., A. Kihara, …, Y. Igarashi. 2006. Intracellular localization and tissue-specific distribution of human and yeast DHHC cysteine-rich domain-containing proteins. *Biochim. Biophys. Acta.* 1761:474–483.

38. Rana, M. S., P. Kumar, …, A. Banerjee. 2018. Fatty acyl recognition and transfer by an integral membrane *S*-acyltransferase. *Science.* 359:eaao6326.

39. Duncan, J. A., and A. G. Gilman. 1996. Autoacylation of G protein alpha subunits. *J. Biol. Chem.* 271:23594–23600.

40. Yang, J., B. Gibson, …, R. W. Gross. 2005. Submicromolar concentrations of palmitoyl-CoA specifically thioesterify cysteine 244 in glyceraldehyde-3-phosphate dehydrogenase inhibiting enzyme activity: a novel mechanism potentially underlying fatty acid induced insulin resistance. *Biochemistry.* 44:11903–11912.

41. Omasits, U., C. H. Ahrens, …, B. Wollscheid. 2014. Protter: interactive protein feature visualization and integration with experimental proteomic data. *Bioinformatics.* 30:884–886.

42. Jennings, B. C., and M. E. Linder. 2012. DHHC protein S-acyltransferases use similar ping-pong kinetic mechanisms but display different acyl-CoA specificities. *J. Biol. Chem.* 287:7236–7245.

43. Rybin, V. O., X. Xu, …, S. F. Steinberg. 2000. *Differential targeting of beta -adrenergic receptor subtypes and adenylyl cyclase to cardiomyocyte caveolae.* A mechanism to functionally regulate the cAMP signaling pathway. *J. Biol. Chem.* 275:41447–41457.

44. Ostrom, R. S., C. Gregorian, …, P. A. Insel. 2001. Receptor number and caveolar co-localization determine receptor coupling efficiency to adenylyl cyclase. *J. Biol. Chem.* 276:42063–42069.

45. Steinberg, S. F., and L. L. Brunton. 2001. Compartmentation of G protein-coupled signaling pathways in cardiac myocytes. *Annu. Rev. Pharmacol. Toxicol.* 41:751–773.

46. Axelrod, D. 1981. Cell-substrate contacts illuminated by total internal reflection fluorescence. *J. Cell Biol.* 89:141–145.

47. Fang, C., L. Deng, …, B. Lüscher. 2006. GODZ-mediated palmitoylation of GABA(A) receptors is required for normal assembly and function of GABAergic inhibitory synapses. *J. Neurosci.* 26:12758–12768.

48. Lai, J., and M. E. Linder. 2013. Oligomerization of DHHC protein S-acyltransferases. *J. Biol. Chem.* 288:22862–22870.

49. Parzen, E. 1962. On estimation of a probability density function and mode. *Ann. Math. Stat.* 33:1065–1076.

50. Rosenblatt, M. 1956. Remarks on some nonparametric estimates of a density function. *Ann. Math. Stat.* 27:832–837.

51. Ohsugi, Y., K. Saito, …, M. Kinjo. 2006. Lateral mobility of membrane-binding proteins in living cells measured by total internal reflection fluorescence correlation spectroscopy. *Biophys. J.* 91:3456–3464.

52. Calebiro, D., F. Rieken, …, M. J. Lohse. 2013. Single-molecule analysis of fluorescently labeled G-protein-coupled receptors reveals complexes with distinct dynamics and organization. *Proc. Natl. Acad. Sci. USA.* 110:743–748.

53. Ma, Y., A. Benda, …, K. Gaus. 2016. Measuring membrane association and protein diffusion within membranes with supercritical angle fluorescence microscopy. *Biomed. Opt. Express.* 7:1561–1576.

54. Qian, H., M. P. Sheetz, and E. L. Elson. 1991. Single particle tracking. Analysis of diffusion and flow in two-dimensional systems. *Biophys. J.* 60:910–921.

55. Rocks, O., A. Peyker, …, P. I. Bastiaens. 2005. An acylation cycle regulates localization and activity of palmitoylated Ras isoforms. *Science.* 307:1746–1752.

56. Goodwin, J. S., K. R. Drake, …, A. K. Kenworthy. 2005. Depalmitoylated Ras traffics to and from the Golgi complex via a nonvesicular pathway. *J. Cell Biol.* 170:261–272.

57. Galbiati, F., F. Guzzi, …, M. Parenti. 1994. N-terminal fatty acylation of the alpha-subunit of the G-protein Gi1: only the myristoylated protein is a substrate for palmitoylation. *Biochem. J.* 303:697–700.

58. Jones, T. L., M. Y. Degtyarev, and P. S. Backlund, Jr. 1997. The stoichiometry of G alpha(s) palmitoylation in its basal and activated states. *Biochemistry.* 36:7185–7191.

59. Martin, B. R., and N. A. Lambert. 2016. Activated G protein Gαs samples multiple endomembrane compartments. *J. Biol. Chem.* 291:20295–20302.

60. Li, Y., J. Hu, …, S. L. Hofmann. 2010. DHHC5 interacts with PDZ domain 3 of post-synaptic density-95 (PSD-95) protein and plays a role in learning and memory. *J. Biol. Chem.* 285:13022–13031.

61. Greaves, J., J. A. Carmichael, and L. H. Chamberlain. 2011. The palmitoyl transferase DHHC2 targets a dynamic membrane cycling pathway: regulation by a C-terminal domain. *Mol. Biol. Cell.* 22:1887–1895.

62. Lin, M. J., M. Fine, …, D. W. Hilgemann. 2013. Massive palmitoylation-dependent endocytosis during reoxygenation of anoxic cardiac muscle. *eLife.* 2:e01295.